American Journal of Pathology, Vol. 169, No. 1, July 2006

DOI: 10.2353/ajpath.2006.060032

Tumorigenesis and Neoplastic Progression

Concurrent Expression of Hyaluronan Biosynthetic and Processing Enzymes Promotes Growth and Vascularization of Prostate Tumors in Mice

Melanie A. Simpson

From the Department of Biochemistry, University of Nebraska, Lincoln, Nebraska

Aggressive cells in prostate cancer secrete extracellular hyaluronan (HA) as a result of up-regulated HA synthase enzymes HAS2 and HAS3. Combined detection of HA and the HA processing hyaluronidase enzyme Hyal1 in prostate tumors correlates with poor outcome. HA oligomers produced by hyaluronidases are potent angiogenic stimuli. We investigated the respective roles of HAS2 and Hyal1 using 22Rv1 human prostate tumor cells that lack both enzyme activities. Stable transfectants were selected for overexpression of Hyal1 or HAS2 and for coexpression of Hyal1 and HAS2. HAS2 overexpression elevated HA production and excess pericellular HA retention. However, HAS2-transfected tumor cell growth in culture was dramatically slowed. Coexpression of Hyal1 with HAS2 diminished HA retention but restored growth kinetics, supporting a possible combined role for excess HA synthesis and processing in maximizing unrestricted growth of prostate cancer cells. In mice, overexpression of HAS2 increased subcutaneous tumor size. Excess activity of either Hyal1 or HAS2 enhanced angiogenesis, but the most significant tumorigenic potential was realized by coexpression of both Hyal1 and HAS2 enzymes. Thus, HA production by tumor cells in prostate cancer may enhance the aggressive potential of the cells by increasing Hyal1-dependent autocrine proliferation and potentiating vascular development. ***(Am J Pathol 2006, 169:247–257; DOI: 10.2353/ajpath.2006.060032)***

Prostate cancer is the second leading cause of cancer death in men.[1] Although treatment efficacy has improved dramatically by increased awareness and earlier diagnosis, a large number of cases progress to aggressive, metastatic disease. Understanding the molecular phenomena that lead to progression would improve diagnostic, prognostic, and therapeutic indices.

A growing body of evidence suggests that aggressive progression of cancer is facilitated by changes in the composition of extracellular matrix surrounding the cancerous tissue. One matrix molecule implicated in the progression of prostate cancer is hyaluronan (HA), a large glycosaminoglycan polymer that is not prominent in normal tissue or benign prostatic hyperplasia but is abundant in tissue biopsies from patients in various stages of prostate cancer.[2–7] Normally, HA is produced during specific events that require cellular proliferation and motility, such as developmental neural crest cell migration,[8] cardiac morphogenesis,[9] prostate development,[10] and wound healing.[11] However, its accumulation is tightly controlled and restricted in adulthood to extracellular matrices within joint tissues, vitreous humor, skin, and protective encapsulation of vital organs.[12,13]

Steady-state levels of HA are maintained by the cumulative efforts of two families of enzymes: the HA synthases[14] (HAS1, HAS2, and HAS3 in mammals) and the hyaluronidases[15] (Hyal1 through Hyal4 and PH20). HA synthases are integral membrane enzymes that synthesize HA polymers of 10^5 to 10^7 d, simultaneously secreting them to the extracellular space as they are polymerized. Retention of HA at the cell surface may result either from association of nascent polymers with the HAS enzyme during actively up-regulated HA synthesis and/or from specific cell-surface HA receptors cross-linking and weaving the polymers into a pericellular matrix.[16–18] Dissolution of HA from the extracellular space requires processing of the polymers into smaller oligomeric units by the hyaluronidases.[19] The respective functions of enzymes and receptors in maintenance of such matrices are not well understood.

Quantitative measurement of HA accumulation in human prostate tumors by histopathological analysis, in

Supported by United States Army grant PC030271, National Institutes of Health (NIH) grant R01-CA106584, and NIH National Center for Research Resources grant P20-RR018759.

Accepted for publication March 28, 2006.

Address reprint requests to Dr. Melanie A. Simpson, Department of Biochemistry, University of Nebraska-Lincoln, N241 Beadle Center, Lincoln, NE 68588-0664. E-mail msimpson2@unl.edu.

combination with elevated expression of the hyaluronidase Hyal1, is an independent indicator of poor prognosis for patients.[5–7] This correlative finding is consistent with studies that show an active role for HA in tumor progression. Overexpression of HA synthases in several cell lines has been shown to stimulate tumorigenicity and metastasis.[20–23] Hyal1 overexpression has been implicated in metastasis[24] and invasive tumor growth,[25] and in glioma cells, excess production of HA requires counterbalance by hyaluronidase expression to promote growth.[26] Hyal1 is a secreted protein found in plasma, urine, and intracellularly in lysosomes.[19] Its activity profile is acidic, suggesting it may function with maximal efficacy in acidic microenvironments such as those created locally within developing tumors. Hyal1 converts polymeric HA to oligomeric species, some of which have potent biological function. Depending on molecular mass, the effect of HA exposure to cells can be antiproliferative (polymeric HA),[27] angiogenic (large HA oligomers),[27–30] or apoptotic (small HA fragments).[31,32] The outcome of concurrent increased HA production and processing on a tumor cell could therefore vary with differential expression of HAS and Hyal isozymes.

Previous studies with human prostate tumor cell lines have shown that excess HA production correlates with aggressive potential of the cell.[33] HAS2 and HAS3 isozymes were found to be specifically up-regulated in the aggressive cells. Inhibition of HAS2 or HAS3 in these cells significantly impairs tumor growth and spontaneous metastatic potential.[34,35] Not surprisingly, HA-deficient tumors are very poorly vascularized relative to HA-rich tumors. However, the respective and concerted roles of hyaluronidase and HA synthase in HA accumulation and utilization by tumor cells have not been examined. In this report, we have selected and characterized prostate tumor cell transfectants for expression of HAS2 or Hyal1 individually and for coexpression of Hyal1/HAS2. Cell lines were compared for enzyme activity, growth properties *in vitro* and *in vivo*, and angiogenic potential in mice. Excess HA production increased cell-surface HA retention and slowed cellular growth dramatically. Interestingly, coexpression of Hyal1 virtually eliminated pericellular HA retention and restored growth rates to control levels. The cotransfected cells exhibited dramatic increases in tumor growth rate on subcutaneous injection. Angiogenesis was stimulated significantly by all three transfection conditions but did not correlate with tumorigenic potential of the cells. This is the first report to begin systematically assessing the roles of HA biosynthesis and degradation in prostate tumor cell biology. The results are consistent with an active role of both processes in progression of prostate cancer.

Materials and Methods

Cell Culture and Reagents

The PC3 derivative cell line, PC3M-LN4 (human prostate adenocarcinoma cells), was kindly provided by Dr. Isaiah J. Fidler (M.D. Anderson Hospital Cancer Center, Houston, TX) and cultured similarly to PC3 in minimal essential medium supplemented with 10% fetal bovine serum, nonessential amino acids, and 1 mmol/L sodium pyruvate. 22Rv1 and LNCaP cells were purchased from the American Type Culture Collection (Manassas, VA) and cultured in Roswell Park Memorial Institute (RPMI) 1640/10% fetal bovine serum as recommended. Biotinylated HA-binding protein (HABP) was from Seikagaku (Northstar BioProducts, Fast Falmouth, MA). HA used in the quantification assay was purchased from Sigma-Aldrich (St. Louis, MO). Anti-mouse CD31-phycoerythrin conjugate was from BD Biosciences (San Diego, CA).

Determination of HAS and Hyaluronidase Expression

Expression of HAS isozymes 1, 2, and 3 was assayed by reverse transcriptase-polymerase chain reaction (RT-PCR) as previously described.[33] Hyal1 in prostate carcinoma cell lines was assayed similarly. Briefly, poly(A)$^+$ RNA was isolated from subconfluent tumor cells (Oligotex mRNA isolation kit; Qiagen, Valencia, CA) and quantified, and equal amounts were reverse-transcribed with an oligo(dT) primer using the Superscript III kit (Invitrogen, Carlsbad, CA). Polymerase chain reaction (PCR) oligonucleotides were designed using the published sequences. Target amplification sequences of 200–400 bases were selected and amplified in 25–35 cycles of 30-seconds denaturation at 95°C, 30-seconds annealing at 60°C, and 30-seconds extension at 72°C. Glyceraldehyde-3-phosphate dehydrogenase was amplified in identical simultaneous reactions as a normalization control. HAS2 expression in stable transfectants was similarly assayed.

Plasmid Construction

The plasmid construct encoding HAS2 was previously described.[34] The Hyal1 coding sequence (accession U96078) was amplified by RT-PCR from PC3M-LN4 cells, subcloned with a Flag epitope tag, and placed in the pIRES2-EGFP bicistronic expression vector (Clontech, Palo Alto, CA) for constitutive expression and antibiotic selection in eukaryotic cells. The sequence was verified for identity to the published sequence. Expression of each coding sequence was confirmed as described below.

Transfection and Stable Selection of Prostate Tumor Cells

22Rv1 human prostate tumor cells were transfected with 1) vector alone (pIRES2-EGFP); 2) plasmid encoding Hyal1-Flag; 3) HAS2 plasmid; or 4) both the Hyal1 and the HAS2 plasmid constructs. Transfections were performed via a liposome-mediated method using FuGene6 reagent (Roche Applied Science, Mannheim, Germany), according to the manufacturer's protocol. Gene expression was verified by RT-PCR (HAS2) or Western blot

(Hyal1) and by enzyme activity assays as described. Stable selection of 22Rv1 transfectants was by clonal isolation with cloning disks following incubation for 14 to 20 days with G418 (1.25 mg/ml). Multiple clones were tested for expression, and those with average levels of expression were pooled to eliminate bias from isolated selection. Once established, stable transfectants were maintained in the selection medium.

Hyaluronidase Activity Assays

Cell culture supernatants from transfected cell lines were concentrated approximately 10-fold and electrophoresed by sodium dodecyl sulfate-polyacrylamide gel electrophoresis on a 12% polyacrylamide gel containing 0.2 mg/ml HA. The gel was soaked for 1 hour at room temperature in 3% Triton X-100 and then incubated in hyaluronidase assay buffer (50 mmol/L sodium formate, pH 4.0, 150 mmol/L NaCl, 0.1% bovine serum albumin (BSA)) at 37°C overnight. Hyaluronidase activity was detected as a clear band at the specific molecular weight (eg, 58 kd) for Hyal1 on staining 1 hour with 0.5% Alcian blue and destaining with 7% acetic acid. Cell lysates were assayed similarly, but, although several light bands were visible, no significant differences were observed between control and Hyal1-transfected cells. Thus, the majority of overexpressed Hyal1 was secreted. To determine whether supernatants or whole cell lysates contained differential activities of the pH neutral hyaluronidases (Hyal2 or PH20), substrate gels generated as above were also assayed in 50 mmol/L sodium phosphate, pH 7.0, containing 150 mmol/L NaCl and 0.1% BSA. No activity was observed in the conditioned media, and, again, several faint bands were present in lysates without significant differences between control and transfected cells. Furthermore, the pattern was not appreciably different between lysates assayed at pH 7 versus pH 4. Hence, these data are not shown.

HA Quantification

The concentration of HA in transfected cell culture supernatants was determined in a competitive binding assay.[36] Briefly, Immulon 96-well microtiter plates were coated with human umbilical cord HA at 50 μg/ml in 200 mmol/L carbonate buffer (pH 9.6) overnight at 4°C. Excess HA was removed, and wells were blocked with Superblock reagent (Pierce, Rockford, IL). Overnight conditioned culture media from prostate tumor cell cultures were harvested, and cell counts were determined manually. Cell culture supernatants were centrifuged, boiled 20 minutes, and serially diluted in phosphate-buffered saline/0.05% Tween 20. Equal volumes of each dilution were combined with biotinylated HABP to a final HABP concentration of 0.5 μg/ml and incubated in the HA-precoated wells at room temperature for 6 to 8 hours. Plates were washed four times with phosphate-buffered saline/Tween 20 and developed using an avidin-biotin horseradish peroxidase system (ABC-HRP kit PK-4000; Vector Laboratories, Burlingame, CA) with tetramethylbenzidine (Sigma-Aldrich) as substrate, and absorbance was read at 650 nm in a PowerWave microplate spectrophotometer (BioTek, Winooski, VT). HA concentration was interpolated from a standard curve of absorbance values corresponding to known HA quantities. The mean HA concentration for each sample of culture supernatant was calculated, and results were normalized to cell number.

HA Pericellular Detection and Quantification

Pericellular HA retention was visualized and quantified by particle exclusion as described previously.[34,35] Briefly, prostate carcinoma cells cultured overnight in 48-well plates were washed and incubated 90 minutes with 2 mg/ml aggrecan in phenol red-free RPMI with 0.1% BSA at 37°C. The aggrecan solution was removed, and 1×10^8 glutaraldehyde-fixed sheep red blood cells (Accurate Chemical and Scientific Corp., Westbury, NY) in phosphate-buffered saline/1% BSA were added, allowed to settle for 15 minutes, and then viewed with phase-contrast microscopy. The HA matrix was evidenced by halos surrounding the cells from which the fixed erythrocytes were excluded. Representative cells were photographed at magnification $\times$400. To quantify matrix retention, outlines of matrices and cellular boundaries from individual cells of each type were traced, and relative areas were calculated using Adobe Photoshop (Adobe Systems Incorporated, San Jose, CA). HA matrix thickness is presented as the ratio of matrix area to cell area for each transfectant or condition, with the mean ratio represented by a horizontal bar.

Growth Assays

Two-dimensional growth in culture was assayed as previously described.[35] Equivalent passages of each tumor cell line were plated at 5000 cells/well in 24-well plates. After 7 days, the most rapidly growing cell line had reached ~90% confluence, so this was chosen as the experimental endpoint. At 24-hour intervals up to 7 days, quadruplicate wells of each cell line were released with trypsin, neutralized, and manually counted in a hemacytometer. Duplicate counts for each well were averaged to obtain the total cell count per well. Each point is the mean $\pm$ SE of the total cell counts. Although the graph presents data from a single assay in quadruplicate, the growth trends were reproduced in three additional identical assays.

Mouse Subcutaneous Injection

All mice were cared for and maintained under the supervision and guidelines of the University of Nebraska-Lincoln Institutional Animal Care and Use Committee. Male non-obese diabetic/severe combined immunodeficient (NOD/SCID) mice (Jackson Laboratories, Bar Harbor, ME, a total of eight animals per condition) were injected subcutaneously in each flank with 1×10^6 tumor cells suspended in 100 μl of serum-free RPMI. Tumor

growth was monitored weekly with caliper measurements. After 28 days, mice were sacrificed, and tumors were dissected and weighed. Mean tumor wet weight ± SE was plotted for each cell line. Statistical significance was assigned by Student's two-tailed *t*-test. The experiment was repeated with an additional eight animals per cell line, and similar results were obtained.

Immunohistochemistry and Immunofluorescence

HA content and vascularization of tumors were detected as described previously.[35] Briefly, after weighing, tumors were divided in halves. One half was formalin-fixed and embedded in paraffin, and the other half was snap frozen in OCT compound. For HA detection, paraffin-embedded tumors were sectioned, dewaxed, incubated with 3 μg/ml biotinylated HABP in phosphate-buffered saline/1% BSA overnight at 4°C, and developed using the Vectastain ABC kit (Vector Laboratories). Sections were counterstained with Meyer's hematoxylin to visualize cellular boundaries. White light images were collected at magnification ×200 on a Leica DM-IRB inverted microscope equipped with an Optronics Magnafire digital camera. Vascularization of the tumors was assessed in acetone-fixed frozen sections (8-μm thickness) by antibody staining for CD31 as described previously.[35,37]

Angiogenesis Quantification

CD31-phycoerythrin-conjugated antibody staining of frozen sections was visualized by fluorescence microscopy. Five random sections from each of three tumors per cell line were digitally photographed with 5-s exposure time, saved as TIF files, and processed. Images were converted from 16 to 8 bit in Adobe Photoshop, red channel fluorescence was specifically isolated, images were converted to grayscale and inverted, and a black-and-white threshold was arbitrarily set based on levels. The histogram function was then used to determine vessel density as represented by density of black pixels at 0 on the black-to-white scale. Average pixel density for each transfectant tumor section was normalized to the average pixel density for untransfected tumor sections. Statistical significance was assigned by Student's two-tailed *t*-test.

Results

22Rv1 Cells Express Hyaluronidases but Lack Significant HA Synthase

To assess the relative and concerted roles of HA biosynthesis and processing, tumor cell lines were first characterized for expression of HA synthase and hyaluronidase isozymes. Hyaluronidases have been reported in aggressive prostate cancer cells,[6,38,39] and expression of the secreted hyaluronidase isozyme Hyal1 appears to correlate directly with human disease progression,[7] as well as with tumorigenic/metastatic behavior in cell lines.[7,24,25] The commercially available human prostate adenocarcinoma cell lines LNCaP, 22Rv1, and PC3, as well as PC3M-LN4 cells, were evaluated for HAS and Hyal expression by RT-PCR. Results showed that mRNA for Hyal1 is expressed in all four cell lines and in normal prostate (Figure 1). Expression was elevated ~2-fold in 22Rv1 cells but was approximately equivalent in LNCaP, PC3, and PC3M-LN4 cells relative to normal prostate (Figure 1, N.Pr.). This observation will be discussed further below. A previous report demonstrated Hyal2 and Hyal3 mRNA expression in PC3 cells.[24] Expression of these messages was detected by RT-PCR at levels that did not differ appreciably among the cell lines tested or in reference to normal prostate (not shown). Hyal2 and Hyal3 proteins have not been implicated functionally in the progression of prostate cancer to date.

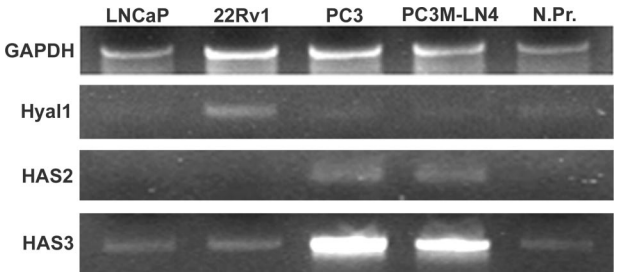

Figure 1. Hyal1 mRNA is expressed in metastatic and non-metastatic prostate carcinoma cells, but only metastatic cells express HAS2 and HAS3. Equivalent amounts of input poly(A)$^+$ RNA from prostate carcinoma cell lines (LNCaP, 22Rv1, PC3, and PC3M-LN4) or a normal prostate mRNA library (N.Pr.) were reverse-transcribed, and target messages were amplified using oligonucleotide primers specific for Hyal1, HAS2, HAS3, or glyceraldehyde-3-phosphate dehydrogenase (housekeeping control) as described previously and in Materials and Methods. An aliquot of 20 μl from each PCR was electrophoresed on a 2% agarose gel and stained with ethidium bromide for digital imaging.

HAS expression was characterized previously for LNCaP, PC3, and PC3M-LN4 cells.[33] LNCaP cells have been used to characterize overexpressed HAS enzymes *in vitro* by transient transfection.[34] However, because these cells do not grow subcutaneously in mice without addition of Matrigel, a reconstituted basement membrane mixture containing HA, an alternative model cell line was sought for stable transfection. Before choosing 22Rv1 for overexpression of the HA metabolic enzymes described in this report, HAS expression was evaluated. Results presented in Figure 1 illustrate a similar expression profile of HAS isozymes for LNCaP, 22Rv1, and normal prostate. HAS2 was not amplified at detectable levels, and HAS3 mRNA was present at detectable but low levels, comparable to normal prostate. Expression of HAS2 and HAS3 was dramatically elevated in PC3 and PC3M-LN4 cells, consistent with the previously published findings. HAS1 was also assayed and, again in accordance with previous results, found not to be expressed at detectable levels. 22Rv1 cells were therefore identified as an appropriate HAS-negative cell line in which to examine the respective roles of the HAS and Hyal1 enzymes.

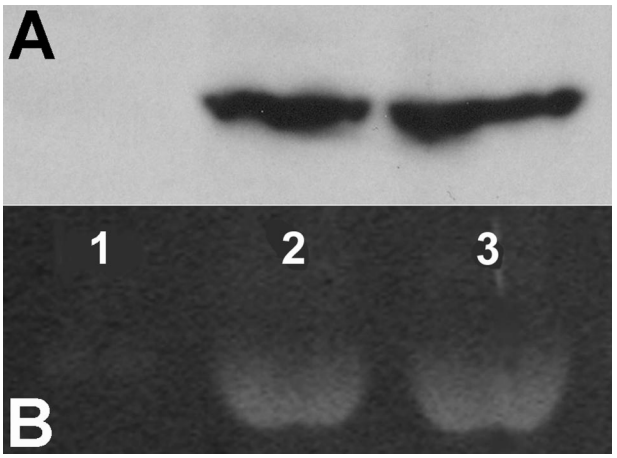

Figure 2. Hyal1 is secreted and active in conditioned media of stable 22Rv1 transfectants. Endogenous hyaluronidase activity and activity encoded by the Hyal1 construct were verified by HA substrate gel electrophoresis. 22Rv1 cells were stably selected for expression of GFP control (**lane 1**), Hyal1 alone (**lane 2**), or combined Hyal1/HAS2 (**lane 3**). **A:** Concentrated media from each cell line were analyzed by Western blot and probed with anti-Flag (2 μg/ml) and developed by ECL. **B:** Concentrated media were electrophoresed on a 12% nonreducing polyacrylamide gel containing 0.2 mg/ml HA. The gel was washed for 1 hour in 3% Triton X-100, incubated in pH 4.0 assay buffer (see Materials and Methods) at 37°C overnight, stained with 0.5% Alcian blue, and destained with 7% acetic acid.

Cloning and Overexpression of Hyaluronidase in 22Rv1 Cells

To overexpress Hyal1 in tumor cells, the full-length Hyal1 cDNA was cloned from PC3M-LN4 cells by RT-PCR using published sequence data. The clone was expressed as a bicistronic message with green fluorescent protein (GFP), with a Flag epitope tag for subsequent immunodetection. Highly expressing transfectants of 22Rv1 cells were selected and pooled. Expression and secretion of Hyal1-Flag specifically in the Hyal1 transfectants was verified by Western blot analysis of conditioned media (Figure 2A). Functional characterization of the secreted Hyal1 enzyme was performed by HA substrate gel electrophoresis for cells stably transfected with control vector (GFP) or Hyal1 cDNA (Figure 2B, lanes 1 and 2). Inspection of the HA substrate gel showed minimal endogenous hyaluronidase activity in concentrated conditioned media from GFP control cultures, despite the apparently elevated mRNA detected by RT-PCR (Figure 1). This may reflect low protein expression or the presence of hyaluronidase inhibitors in the culture serum.[40] Similar assay of culture media from Hyal1 transfectants (lane 2) shows that the Hyal1 clone is not only expressed and secreted at the 58-kd molecular weight previously reported for active Hyal1 but is enzymatically active. No other major bands were visible, suggesting no other detectable hyaluronidase activity was secreted by 22Rv1 cells. The Western blot and the substrate gel indicated that both expression and enzyme activity are comparable in conditioned media from tumor cells that have been selected for stable expression of Hyal1 alone (lane 2) or coexpression of Hyal1 and HAS2 (lane 3). Because overexpression of Hyal1 has been shown to have a dose-dependent effect on tumorigenesis in mice with extremely high levels

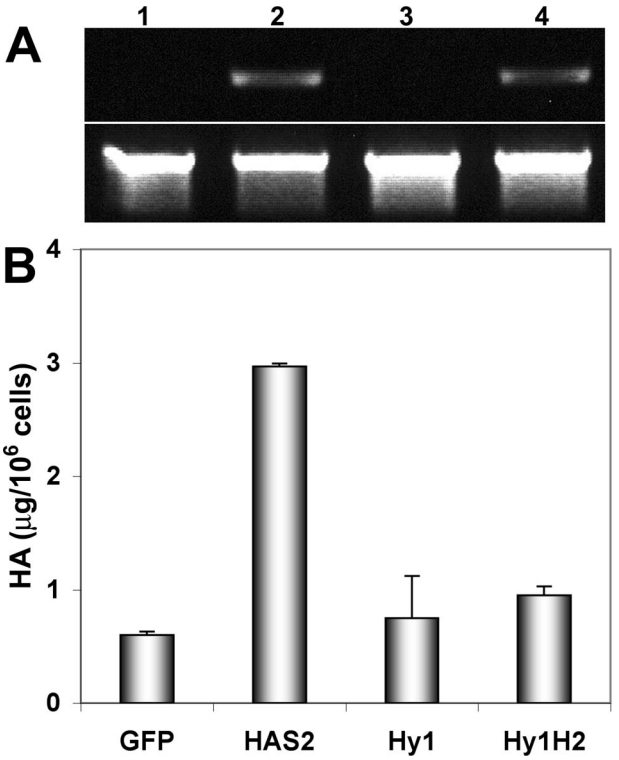

Figure 3. HA production is enhanced in HAS transfectants. **A:** Expression of HAS2 mRNA in 22Rv1 cells stably selected for GFP control (**lane 1**), HAS2 (**lane 2**), Hyal1 (**lane 3**), or Hyal1 plus HAS2 (**lane 4**) was assayed semiquantitatively by RT-PCR (**upper panel**) with glyceraldehyde-3-phosphate dehydrogenase amplified as a normalization control (**lower panel**). **B:** HA content of conditioned media was quantified by competitive binding as described in Materials and Methods and normalized to cell count. The mean value ± SE is plotted for each cell line assayed in triplicate serial dilutions.

actually suppressing tumor growth,[25] it was especially important to normalize enzyme activities.

Overexpression of HA Synthases and Coexpression with Hyaluronidase

In addition to Hyal1-stable transfectants, 22Rv1 cells were also selected and characterized for stable expression of HAS2. HAS2 expression in transfected cells was semiquantitatively assessed by RT-PCR (Figure 3A, lanes 2 and 4). Functionality of the overexpressed HAS2 enzyme was assessed in transfectants by measuring HA content of conditioned media from control and HAS2 cultures (Figure 3B). GFP controls produced very little HA, consistent with results of HA analysis of the untransfected 22Rv1 cell line (not shown) and with the low detectable HAS mRNA in both untransfected (Figure 1) or GFP-transfected (Figure 3A, lane 1) 22Rv1 cells. Stably selected HAS2 lines were characterized for HA production as shown in Figure 3B. HAS2 transfectants produced >5-fold more HA than the GFP controls, indicating the enzyme is expressed and active in 22Rv1 cells, which clearly have the capacity to produce HA (ie, they synthesize the requisite UDP-sugar precursors), although they poorly express the HAS enzymes.

Additional populations of stable 22Rv1 transfectants were selected and characterized for coexpression of

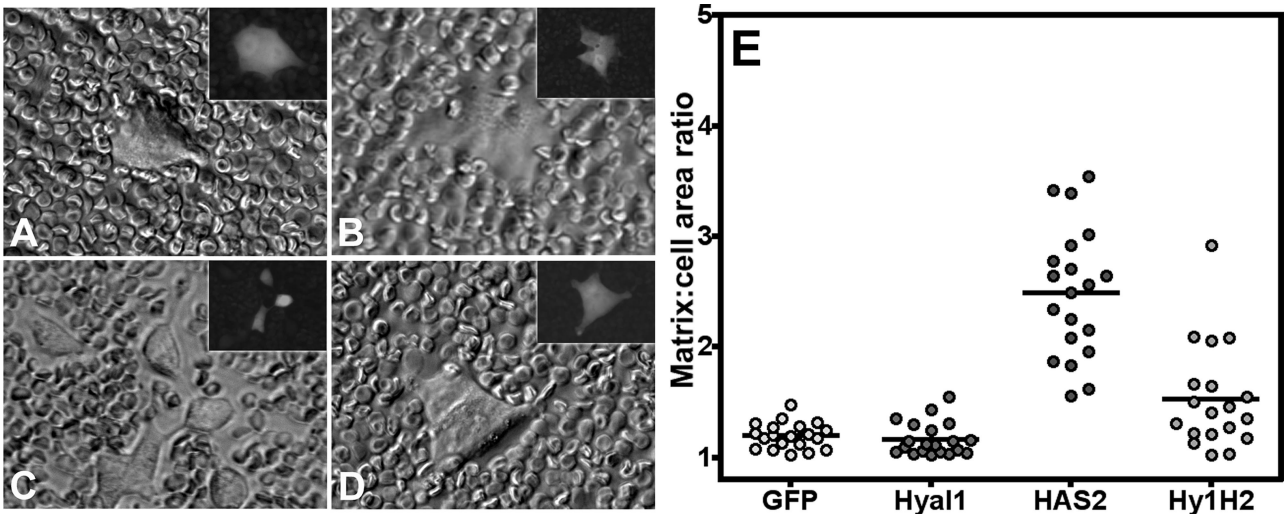

Figure 4. Stable HAS overexpression in 22Rv1 cells confers pericellular HA matrix retention only in the absence of significant hyaluronidase activity. HA pericellular matrix retention of the stably selected cell lines was evaluated by particle exclusion. Overnight cultures of 22Rv1 cells selected for expression of GFP control vector (**A**), Hyal1 alone (**B**), HAS2 alone (**C**), and concurrent Hyal1/HAS2 (**D**) were incubated with 2 mg/ml aggrecan for 90 minutes. After washing, 1×10^8 fixed erythrocytes were added to each culture and allowed to settle. Clear zones around clusters of HAS2 transfectants indicate the presence of HA. GFP reporter expression in each representative cell is shown in the corresponding **inset**. To quantify HA retention, matrix and surface boundaries of 20 individual cells per transfected line were traced in Adobe Photoshop to obtain relative areas in pixels. Area ratios were plotted as a distribution of values for each individual cell (**E**), with the mean represented by a horizontal bar.

Hyal1 and HAS2 enzymes. Figure 2 illustrates equivalent Hyal1 expression and activity in conditioned media from Hyal1 (lane 2) and Hyal1/HAS2 (lane 3) cells. However, in Figure 3B, HA content of the Hyal1/HAS2 cotransfectant media is shown to be reduced almost to normal levels despite equivalent expression of HAS2 relative to the HAS2-only transfectants (compare Figure 3A, lanes 2 and 4). This is likely attributable to limitations in the detection method, which depends on high affinity binding to an HA-binding protein that only recognizes the polymers. Because the Hyal1 and HAS expression levels are equivalent in single transfectants and cotransfectants, it is reasonable to assume HA is degraded as it is synthesized in the cotransfected cells.

Highly expressing clones were characterized for HA-surface retention by particle exclusion (Figure 4). As expected, GFP control transfectants (Figure 4A) retained no detectable cell-surface HA, consistent with their lack of HAS expression. Not surprisingly, transfection with Hyal1 did not confer the potential to retain surface HA, although the cellular morphology was slightly flattened such that cell boundaries became more difficult to distinguish (Figure 4B). By contrast, HAS2-transfected 22Rv1 cells retained abundant surface HA, evident as pericellular clear zones in the images (Figure 4C). Inset panels represent fluorescence images of the same cell to outline the cell boundary and illustrate approximately equivalent levels of GFP reporter expression among all of the clones. Interestingly, HA was present on the surface of Hyal1/HAS2 cotransfected cells (Figure 4D), but its retention was diminished.

To illustrate levels of HA retention in a quantitative fashion, matrix and cell boundaries of 20 randomly selected individual cells from each transfected line were traced in Adobe Photoshop. Areas for each were determined and plotted as a ratio (Figure 4E); a value of 1 indicates no detectable matrix. HAS2 transfectants were encircled with significantly larger clear zones than control, Hyal1-, or Hyal1/HAS2-transfected cells. Because HAS expression was equivalent for the HAS2 and Hyal1/HAS2 cell lines (Figure 3A), this observation suggests that HA is degraded and released from the cell surface by Hyal1 in the cotransfectants. Analysis of HA secretion by the respective cell lines also demonstrated reduced HA quantities present in Hyal1/HAS2 cotransfectant-conditioned media relative to HAS alone (Figure 3B), which is again consistent with the average product size of complete Hyal1-mediated HA degradation (tetra- and hexasaccharides) not detected by this assay.

HAS Overexpression Slows Intrinsic Growth Rate of 22Rv1 Cells

As a prelude to animal studies, growth properties of the 22Rv1-stable transfectants were measured *in vitro*. To assay intrinsic growth rate in standard two-dimensional cell culture conditions, stable transfectants were seeded in equal numbers, grown in serum-containing medium, and counted manually following trypsin release each day for 7 days. Growth rate of Hyal1 transfectants was somewhat faster than that of GFP controls (Figure 5). In contrast, HAS2 transfectants were significantly slower growing, suggesting overproduction of HA actually slowed growth of cells in culture. Because addition of exogenous HA at concentrations up to 1 mg/ml had no effect on growth of the control cells (not shown), the slowed growth was apparently limited to cells that were selected to produce HA. Interestingly, coexpression of HAS2 with Hyal1 restored growth to control levels.

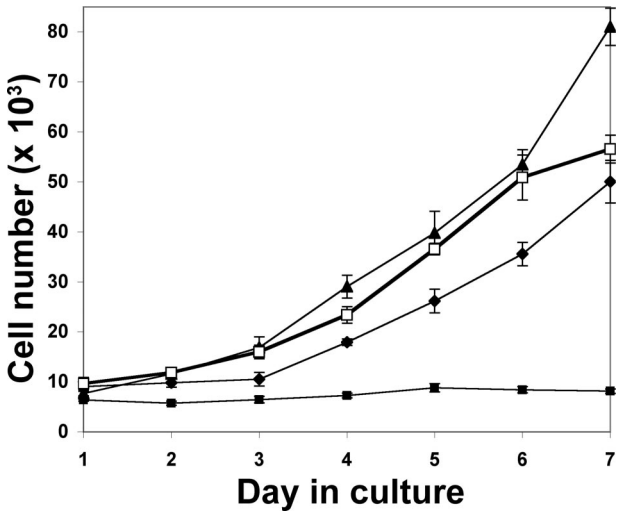

Figure 5. *In vitro* growth of 22Rv1 cells is slowed by stable expression of HAS but restored by coexpression of HAS with Hyal1. Quadruplicate wells of stable transfectants (5000 cells/well of a 24-well plate) were seeded in serum-containing RPMI. Cells were released and counted manually each day as indicated. Data points indicate the mean ± SE. Growth curves are plotted for GFP controls (**diamonds**), individual Hyal1 (**triangles**), and HAS2 (**filled squares**) transfectants, and Hyal1/HAS2 (**open squares**) cotransfectants.

Overexpression of HAS2 and Coexpression of HAS2 with Hyal1 Promotes Tumorigenesis and Angiogenesis

Tumor-forming potential of the stable transfectants was assayed by subcutaneous injection (1×10^6 cells) into flanks of male NOD/SCID mice. After 4 weeks, mice were sacrificed, tumors were weighed, tumor appearance was assessed, and tissue was both cryopreserved for subsequent angiogenesis quantification and formalin-fixed for hematoxylin/eosin staining and HA detection. Tumor weights are plotted in Figure 6A. Consistent with the reported phenotype, the 22Rv1 control GFP-transfected cells were moderately tumorigenic,[41] and the tumor appearance was quite avascular. Hyal1 transfectants gave rise to similarly sized tumors, but differences in vascularity were macroscopically visible (Figure 6B) with the consistency of the tissue altered: rather than firm, encapsulated tissue, these tumors were very soft and difficult to palpate. Despite their slow intrinsic growth rate, HAS2-transfected cells produced somewhat larger tumors that were also highly vascular. Tumor take in these animals was ~50%, in contrast to 100% for the other cell lines in the study, so the overall significance of altered tumor size was difficult to establish. However, the injections were repeated several times with the average tumor size of HAS2 transfectants consistently twofold larger than GFP controls ($P = 0.116$ for the representative data shown in Figure 6) or the Hyal1 transfectants ($P = 0.038$). Coexpressing Hyal1/HAS2 tumors were among the largest obtained from subcutaneous injections of prostate tumor cells. The mean tumor size was approximately threefold larger than GFP controls ($P = 0.010$) and ~50% larger than the average size of HAS2 tumors, although this was again difficult to show statistically ($P = 0.101$). The ex-

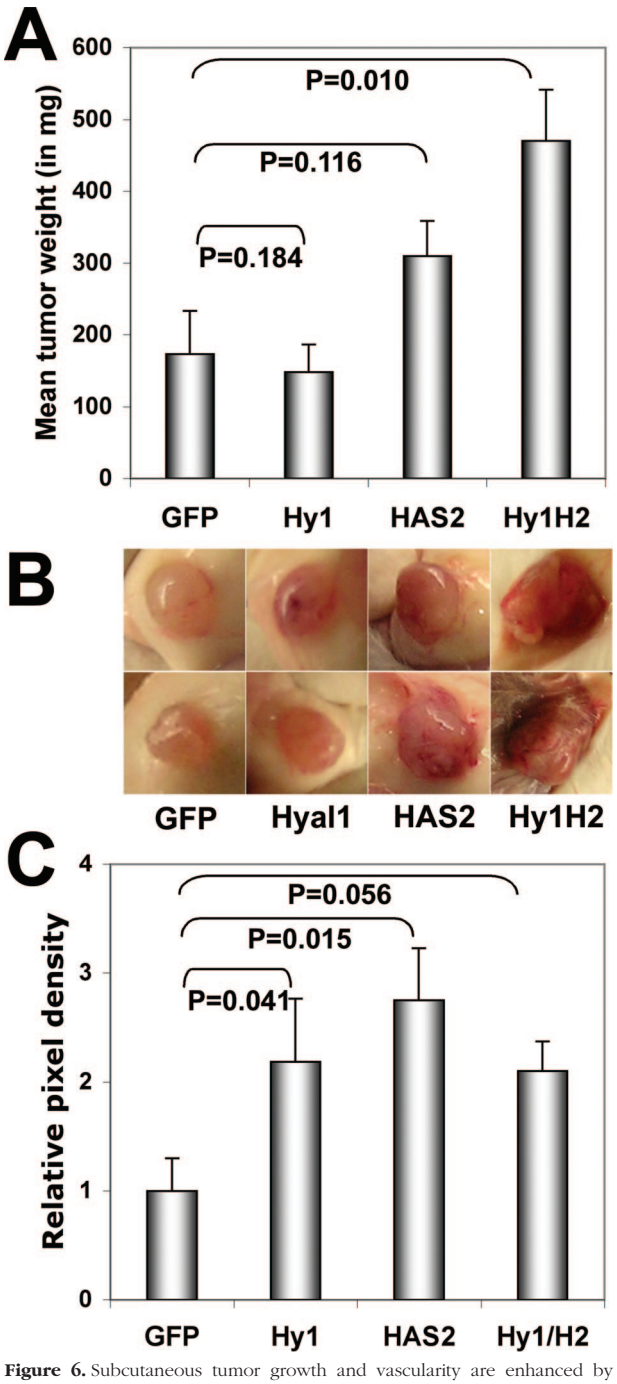

Figure 6. Subcutaneous tumor growth and vascularity are enhanced by HAS2 and Hyal1/HAS2 overexpression. Stably transfected 22Rv1 cells were trypsin-released and resuspended in serum-free RPMI. Male NOD/SCID mice were injected subcutaneously in each flank with 1×10^6 tumor cells. At 4 weeks after injection, tumors were excised, weighed, and preserved for tissue sectioning. **A:** Mean tumor wet weight ± SE is plotted for each transfected cell line. Statistical significance determined by Student's two-tailed *t*-test is indicated on the graph for each cell line relative to the control (GFP). **B:** Tumors generated by each cell line were photographed *in situ*. Duplicate representative tumors from each group illustrate macroscopic differences in surface vascularity that correlate with HAS2 overexpression. **C:** Triplicate cryosections from three tumors per cell line were stained with anti-CD31-phycoerythrin to visualize vascular endothelial cells. Five random digital images per section were captured on a fluorescence microscope and processed as described in Materials and Methods. Mean relative pixel density ± SE for all images within a group is plotted as a measure of tumor vasculature with respect to identically processed tumors from the parental 22Rv1 cell line. Statistical significance, determined by *t*-test, is indicated on the graph for each cell line relative to the control (GFP). Additional statistics are discussed in the text.

ternal vascular appearance of these tumors surpassed that of the individual transfectants, and the architecture of the tumors was compromised (soft) as it was for Hyal1 tumors.

Vascular density of the tumors was assessed quantitatively as described previously. The tumors were cryosectioned and stained for the endothelial cell-specific surface receptor CD31 using a phycoerythrin-conjugated antibody for immunofluorescence. Digital images were processed to determine vessel density in the tumor sections, which was plotted as relative pixel density averaged among all tumor images (Figure 6C). The graph illustrates a correlation between the increased tumor size of the HAS2 ($P = 0.015$) and Hyal1/HAS2 ($P = 0.056$) tumors and increased vascularization. However, Hyal1 tumors also had significantly higher vessel density than controls ($P = 0.041$), despite comparable tumor size. Hyal1 expression alone, although stimulating angiogenesis, was not sufficient to promote enhanced tumorigenesis.

Finally, the HA content of the tumors was determined histochemically using labeled HA-binding protein (Figure 7). As expected by *in vitro* analysis of the cell lines, virtually no HA was detectable in tumor sections derived from the GFP control (Figure 7A) or Hyal1-transfected (Figure 7B) 22Rv1 cell lines. In contrast, HA accumulation was significant in tumors arising from injection of HAS2 transfectants, as evidenced by the strong brown precipitate (Figure 7C). Consistent with reduced apparent detection of HA secretion in culture, Hyal1/HAS2 tumors also contained very little HA, although there was a slight increase in deposition relative to control GFP tumors (Figure 7D). Collectively, these results may support a model in which the production of HA stimulates tumorigenesis, but this enhanced growth potential is maximal if the HA is also processed in the environment of the tumor. The source of the processing enzyme may be the tumor cell itself or cells residing in the environment to which the tumor cell is introduced.

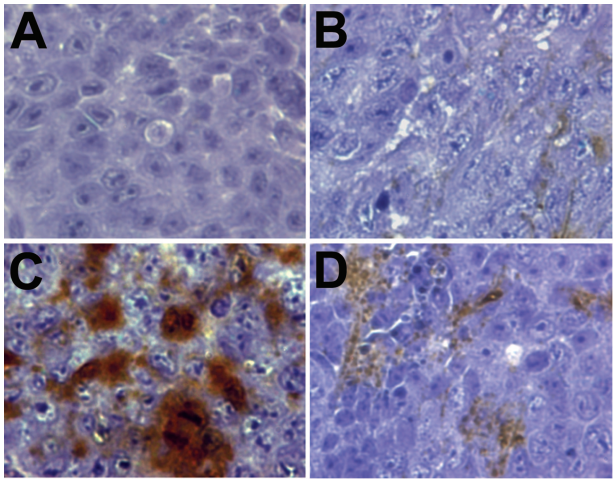

Figure 7. HA content of subcutaneous tumors. Formalin-fixed, paraffin-embedded tumors were sectioned and stained with biotinylated HABP to visualize HA content. Presence of HA is indicated by a brown precipitate. Hematoxylin counterstain illustrates cellular boundaries. Representative sections photographed on an inverted light microscope at magnification ×400 are shown from GFP control (**A**), Hyal1 (**B**), HAS2 (**C**), and Hyal1/HAS2 (**D**) tumors.

Discussion

Aggressive prostate tumor cells produce abundant HA and retain it at the cell surface. This property stems at least in part from the overexpression of HA synthases HAS2 and HAS3. However, the exogenous addition of HA to HAS-inhibited tumor cells is sufficient to restore the diminished *in vivo* growth and vascularization of those cells. Because it is unlikely the HA remains associated with those cells for long, the cells must express additional proteins that stimulate proliferation and vascular endothelial cell recruitment. HA processing and internalization have been shown to promote these processes, so the HA-processing enzymes, hyaluronidases, are likely candidates for growth promoters in the presence of HA. In this study, the respective roles of HA synthase and the prostate tumor cell-secreted hyaluronidase Hyal1 were systematically addressed in stable transfectants that expressed little endogenous HA metabolic activity. HA produced by HAS2 was significantly growth inhibitory *in vitro* unless Hyal1 was coexpressed, supporting a combined role of excess HA synthesis and processing in maximizing unrestricted growth of prostate cancer cells. Excess activity of either Hyal1 or HAS2 enhanced angiogenesis in subcutaneous tumors, but the most significant tumorigenic potential was realized by coexpression of both enzymes. The results are consistent with previous findings that implicate each enzyme independently in prostate tumor progression, but this is the first report to investigate the combined roles of HA synthesis and processing.

HA is a critical mediator of cellular behavior during normal development.[42–44] Mitotic cells deposit HA during cell rounding and separation, leading to the hypothesis that HA may facilitate transient release from adhesion constraints for the purpose of cell division.[45] For example, HA is required for motility of neural crest cells during embryogenesis,[8] as well as for prostate epithelial cells during ductal branching in the developing prostate.[10] In cardiac development, HA not only provides a substrate for migration of pericardial endothelial cells but also stimulates an epithelial to mesenchymal transition, which converts these cells to a motile phenotype.[9] These observations underscore the importance of HA as a specific biological stimulus, production of which must be closely controlled by the concerted effects of HA synthases and hyaluronidases.

HA has been extensively implicated in pathologies such as cancer in which its dysregulated metabolism promotes cellular transformation, proliferation, and motility. The pathological consequences of excess HA production have been demonstrated by overexpression of the HAS enzymes in several cell types. Transfection of mammary carcinoma,[21] fibrosarcoma,[22] or melanoma cells[46] with HAS1 or HAS2 confers enhanced tumorigenesis or metastasis in mice. Studies in mice have also shown that inhibition of HAS2 or HAS3 decreases HA

production and reduces the tumorigenic potential of the cells.[35,47] The effect of HA on tumorigenesis was recently found to be concentration-dependent. Stable lines selected for different levels of HA production by HAS1 overexpression were proportionally more tumorigenic when synthesizing moderate amounts of HA, but tumor growth was inhibited somewhat in cells that produced excessive quantities.[48] In this report, we selected HAS2 cell lines that produce HA at tumor-promoting levels. Additionally, overexpression of HAS2 alone was shown to be sufficient to enhance the tumorigenic potential of prostate tumor cells, although this effect may be dependent on a hyaluronidase-rich microenvironment such as the subcutaneum. The HAS2 gene is located in a region of DNA on chromosome 8 (8q24) that has been found overrepresented by a genetic translocation in human prostate cancer biopsies, correlating to progression.[49] Thus, it is intriguing to speculate that one consequence of this genetic lesion may be the promotion of tumorigenesis by elevation of HA synthesis in neoplasia.

Interestingly, HA production inhibited growth of tumor cells in culture. HA has been shown to associate with the mitotic spindle during cell division,[50,51] so its elevated production may interfere with mitosis or limit the physical separation of newly divided cells. Coexpression of HAS2 with Hyal1 was able to restore growth, which could both serve to release the cells physically and to facilitate endosomal internalization of HA. In fact, induction of Hyal1 in tumor cells has been previously shown by cell-cycle analysis to increase the number of cells in mitosis.[52] This cellular response to HA oligosaccharides appears to require internalization, mediated by ligation of HA to specific cell-surface receptors and the subsequently engaged endosomal mechanisms.[53] Direct interactions between ligated HA receptors and intracellular effector proteins may provide a stimulus for ras transformation and proliferation,[9,53] as well as transducing signals that increase cell motility. In contrast, HA polymers of the size produced by HAS enzymes, when administered exogenously to cells or animals, have been shown to have an antiproliferative and antiangiogenic effect.[27,28] HA oligomers can influence cell behavior by competitively displacing ligated HA polymers, thereby disrupting locally clustered receptors and transmitting signals for proliferation and motility. Hyal1 may thus restore the rapid growth of HAS-overexpressing cells by providing HA oligomers that stimulate proliferation.

The creation of processed fragments with the capacity to induce proliferative, angiogenic, motile, or apoptotic responses depends on the hyaluronidases. Hyaluronidase isozymes are expressed in a tissue-specific manner and exhibit differential subcellular localization.[19] The most well characterized isozyme, PH20, is testicular specific and linked to the cell surface by a glycosylphosphatidylinositol anchor. Hyal2 is fairly ubiquitous, has comparatively low hyaluronidase activity, and is glycosylphosphatidylinositol-anchored. Hyal1 is a secreted protein abundant in plasma and urine. It is postulated that Hyal1 and Hyal2 function in concert and/or in tandem to facilitate HA turnover and subsequent endosomal internalization of HA, for lysosomal degradation and/or stimulation of proliferation signaling cascades.[54–56] Hyaluronidases degrade HA to smaller polymers of 3 to 20 kd or to oligosaccharide fragments of 4 to 6 saccharide units. Overexpression of PH20 in human melanoma cell lines induces vascularization of tumors formed in a mouse corneal model,[57] suggesting the HA oligosaccharide product of the enzyme is angiogenic. HA oligosaccharides have demonstrated angiogenic activity whether administered *in vitro*[29] or systemically in mice.[58] These small fragments of HA are considered to be biologically active in recruitment of endothelial cells, particularly during angiogenesis.[27,28,30,59] Hyal1 overexpressed in prostate tumor cells enhances metastatic potential in mice,[24] possibly through increased vascularity. However, neither of these studies investigated the role of HA biosynthesis. In our experiments, Hyal1 was expressed without a source of HA other than the microenvironment of the subcutaneum and was found to promote angiogenesis without any effect on tumorigenesis. This suggests that HA must be tumor cell-associated to stimulate tumor cell proliferation, but Hyal1 can act on nearby endothelial cells bearing their own surface HA, thus triggering endothelial cell motility and/or proliferation.

Recently, it has been suggested that overproduction of HA via up-regulated synthesis is insufficient to bestow increased growth properties on cells and that HAS overexpression is tumorigenic only in cell types that also express hyaluronidase.[26] Elevated expression of both HAS2 and Hyal2 has recently been found to correlate with aggressive human breast cancers.[47,60] Mechanistically, these observations have not been investigated. In this report, coexpression of HAS2 and Hyal1 restored the growth rate of prostate tumor cells that had been impaired by expression of HAS2 alone. This effect supports a model in which excess HA production leads to surface HA accumulation that inhibits cell proliferation, possibly by stalling mitosis or by physically limiting cellular division, unless a processing enzyme is present to facilitate turnover. Hyaluronidase enzyme activity may actually be inhibited by excess HA,[61] so turnover would be slow in these cells. Concurrently expressed Hyal1 would thus promote turnover of HA for provision of a sustained proliferation stimulus. It is notable that restoration of growth can also be achieved by supplementing the culture medium of the cells with exogenous hyaluronidase (data not shown). In culture, the effect of hyaluronidase coexpression or addition is not significantly different from that of controls, but in mice it is considerable. In this environment, the elevated HA may be an advantage to the early and continued development of the tumor, by facilitating continual cellular proliferation in an autocrine fashion and by promoting blood vessel formation to sustain the tumor.

In conclusion, we have investigated the respective roles of Hyal1 and HAS2 in determining cellular growth rate and tumorigenic and angiogenic potential in a prostate cancer model. Stable overexpressing lines were also used to assess maintenance of cell-surface HA, which we have previously found to correlate with tumorigenesis and metastasis in mice following subcutaneous or orthotopic injection. It is evident from this study that tumorigenic potential alone does not correlate with cell-surface

HA retention, because the coexpression of HAS2 and Hyal1 caused little HA to be retained by the cells but maximally enhanced tumor growth. We are currently investigating the roles of these enzymes in orthotopic growth and metastasis. The results described here support a complex role for both HA biosynthesis and processing by HAS and Hyal, respectively, in conferring aggressive phenotype to otherwise relatively nonaggressive cells.

Acknowledgments

I thank Katherine Metz, Kimberly Hansen, and Christian Elowsky for excellent technical assistance and Joe Barycki for critical evaluation of the manuscript.

References

1. Landis SH, Murray T, Bolden S, Wingo PA: Cancer statistics, 1999. CA Cancer J Clin 1999, 49:8–31
2. Aaltomaa S, Lipponen P, Tammi R, Tammi M, Viitanen J, Kankkunen JP, Kosma VM: Strong stromal hyaluronan expression is associated with PSA recurrence in local prostate cancer. Urol Int 2002, 69:266–272
3. De Klerk DP: The glycosaminoglycans of normal and hyperplastic prostate. Prostate 1983, 4:73–81
4. De Klerk DP, Lee DV, Human HJ: Glycosaminoglycans of human prostatic cancer. J Urol 1984, 131:1008–1012
5. Ekici S, Cerwinka WH, Duncan R, Gomez P, Civantos F, Soloway MS, Lokeshwar VB: Comparison of the prognostic potential of hyaluronic acid, hyaluronidase (HYAL-1), CD44v6 and microvessel density for prostate cancer. Int J Cancer 2004, 112:121–129
6. Lokeshwar VB, Rubinowicz D, Schroeder GL, Forgacs E, Minna JD, Block NL, Nadji M, Lokeshwar BL: Stromal and epithelial expression of tumor markers hyaluronic acid and HYAL1 hyaluronidase in prostate cancer. J Biol Chem 2001, 276:11922–11932
7. Posey JT, Soloway MS, Ekici S, Sofer M, Civantos F, Duncan RC, Lokeshwar VB: Evaluation of the prognostic potential of hyaluronic acid and hyaluronidase (HYAL1) for prostate cancer. Cancer Res 2003, 63:2638–2644
8. Fujimoto T, Hata J, Yokoyama S, Mitomi T: A study of the extracellular matrix protein as the migration pathway of neural crest cells in the gut: analysis in human embryos with special reference to the pathogenesis of Hirschsprung's disease. J Pediatr Surg 1989, 24:550–556
9. Camenisch TD, Spicer AP, Brehm-Gibson T, Biesterfeldt J, Augustine ML, Calabro A Jr, Kubalak S, Klewer SE, McDonald JA: Disruption of hyaluronan synthase-2 abrogates normal cardiac morphogenesis and hyaluronan-mediated transformation of epithelium to mesenchyme. J Clin Invest 2000, 106:349–360
10. Gakunga P, Frost G, Shuster S, Cunha G, Formby B, Stern R: Hyaluronan is a prerequisite for ductal branching morphogenesis. Development 1997, 124:3987–3997
11. Yung S, Thomas GJ, Davies M: Induction of hyaluronan metabolism after mechanical injury of human peritoneal mesothelial cells in vitro. Kidney Int 2000, 58:1953–1962
12. Fraser JR, Laurent TC, Laurent UB: Hyaluronan: its nature, distribution, functions and turnover. J Intern Med 1997, 242:27–33
13. Laurent TC, Laurent UB, Fraser JR: The structure and function of hyaluronan: an overview. Immunol Cell Biol 1996, 74:A1–A7
14. Weigel PH, Hascall VC, Tammi M: Hyaluronan synthases. J Biol Chem 1997, 272:13997–14000
15. Csoka AB, Frost GI, Stern R: The six hyaluronidase-like genes in the human and mouse genomes. Matrix Biol 2001, 20:499–508
16. Toole BP: Hyaluronan promotes the malignant phenotype. Glycobiology 2002, 12:37R–42R
17. Toole BP: Hyaluronan: from extracellular glue to pericellular cue. Nat Rev Cancer 2004, 4:528–539
18. Day AJ, de la Motte CA: Hyaluronan cross-linking: a protective mechanism in inflammation? Trends Immunol 2005, 26:637–643
19. Menzel EJ, Farr C: Hyaluronidase and its substrate hyaluronan: biochemistry, biological activities and therapeutic uses. Cancer Lett 1998, 131:3–11
20. Itano N, Atsumi F, Sawai T, Yamada Y, Miyaishi O, Senga T, Hamaguchi M, Kimata K: Abnormal accumulation of hyaluronan matrix diminishes contact inhibition of cell growth and promotes cell migration. Proc Natl Acad Sci USA 2002, 99:3609–3614
21. Itano N, Sawai T, Miyaishi O, Kimata K: Relationship between hyaluronan production and metastatic potential of mouse mammary carcinoma cells. Cancer Res 1999, 59:2499–2504
22. Kosaki R, Watanabe K, Yamaguchi Y: Overproduction of hyaluronan by expression of the hyaluronan synthase Has2 enhances anchorage-independent growth and tumorigenicity. Cancer Res 1999, 59:1141–1145
23. Liu N, Gao F, Han Z, Xu X, Underhill CB, Zhang L: Hyaluronan synthase 3 overexpression promotes the growth of TSU prostate cancer cells. Cancer Res 2001, 61:5207–5214
24. Patel S, Turner PR, Stubberfield C, Barry E, Rohlff CR, Stamps A, McKenzie E, Young K, Tyson K, Terrett J, Box G, Eccles S, Page MJ: Hyaluronidase gene profiling and role of hyal-1 overexpression in an orthotopic model of prostate cancer. Int J Cancer 2002, 97:416–424
25. Lokeshwar VB, Cerwinka WH, Isoyama T, Lokeshwar BL: HYAL1 hyaluronidase in prostate cancer: a tumor promoter and suppressor. Cancer Res 2005, 65:7782–7789
26. Enegd B, King JA, Stylli S, Paradiso L, Kaye AH, Novak U: Overexpression of hyaluronan synthase-2 reduces the tumorigenic potential of glioma cells lacking hyaluronidase activity. Neurosurgery 2002, 50:1311–1318
27. West DC, Kumar S: The effect of hyaluronate and its oligosaccharides on endothelial cell proliferation and monolayer integrity. Exp Cell Res 1989, 183:179–196
28. West DC, Kumar S: Hyaluronan and angiogenesis. Ciba Found Symp 1989, 143:187–201, discussion 201–187, 281–285
29. West DC, Hampson IN, Arnold F, Kumar S: Angiogenesis induced by degradation products of hyaluronic acid. Science 1985, 228:1324–1326
30. West DC, Kumar S: Tumour-associated hyaluronan: a potential regulator of tumour angiogenesis. Int J Radiat Biol 1991, 60:55–60
31. Ghatak S, Misra S, Toole BP: Hyaluronan oligosaccharides inhibit anchorage-independent growth of tumor cells by suppressing the phosphoinositide 3-kinase/Akt cell survival pathway. J Biol Chem 2002, 277:38013–38020
32. Ward JA, Huang L, Guo H, Ghatak S, Toole BP: Perturbation of hyaluronan interactions inhibits malignant properties of glioma cells. Am J Pathol 2003, 162:1403–1409
33. Simpson MA, Reiland J, Burger SR, Furcht LT, Spicer AP, Oegema TR Jr, McCarthy JB: Hyaluronan synthase elevation in metastatic prostate carcinoma cells correlates with hyaluronan surface retention, a prerequisite for rapid adhesion to bone marrow endothelial cells. J Biol Chem 2001, 276:17949–17957
34. Simpson MA, Wilson CM, Furcht LT, Spicer AP, Oegema TR Jr, McCarthy JB: Manipulation of hyaluronan synthase expression in prostate adenocarcinoma cells alters pericellular matrix retention and adhesion to bone marrow endothelial cells. J Biol Chem 2002, 277:10050–10057
35. Simpson MA, Wilson CM, McCarthy JB: Inhibition of prostate tumor cell hyaluronan synthesis impairs subcutaneous growth and vascularization in immunocompromised mice. Am J Pathol 2002, 161:849–857
36. Frost GI, Stern R: A microtiter-based assay for hyaluronidase activity not requiring specialized reagents. Anal Biochem 1997, 251:263–269
37. Wild R, Ramakrishnan S, Sedgewick J, Griffioen AW: Quantitative assessment of angiogenesis and tumor vessel architecture by computer-assisted digital image analysis: effects of VEGF-toxin conjugate on tumor microvessel density. Microvasc Res 2000, 59:368–376
38. Lokeshwar VB, Lokeshwar BL, Pham HT, Block NL: Association of elevated levels of hyaluronidase, a matrix-degrading enzyme, with prostate cancer progression. Cancer Res 1996, 56:651–657
39. Madan AK, Pang Y, Wilkiemeyer MB, Yu D, Beech DJ: Increased hyaluronidase expression in more aggressive prostate adenocarcinoma. Oncol Rep 1999, 6:1431–1433

40. Mio K, Stern R: Inhibitors of the hyaluronidases. Matrix Biol 2002, 21:31–37
41. Sramkoski RM, Pretlow TG II, Giaconia JM, Pretlow TP, Schwartz S, Sy MS, Marengo SR, Rhim JS, Zhang D, Jacobberger JW: A new human prostate carcinoma cell line, 22Rv1. In Vitro Cell Dev Biol Anim 1999, 35:403–409
42. Delpech B, Girard N, Bertrand P, Courel MN, Chauzy C, Delpech A: Hyaluronan: fundamental principles and applications in cancer. J Intern Med 1997, 242:41–48
43. Laurent TC, Laurent UB, Fraser JR: Serum hyaluronan as a disease marker. Ann Med 1996, 28:241–253
44. Toole BP: Hyaluronan in morphogenesis. J Intern Med 1997, 242:35–40
45. Evanko SP, Angello JC, Wight TN: Formation of hyaluronan- and versican-rich pericellular matrix is required for proliferation and migration of vascular smooth muscle cells. Arterioscler Thromb Vasc Biol 1999, 19:1004–1013
46. Zhang L, Underhill CB, Chen L: Hyaluronan on the surface of tumor cells is correlated with metastatic behavior. Cancer Res 1995, 55:428–433
47. Udabage L, Brownlee GR, Waltham M, Blick T, Walker EC, Heldin P, Nilsson SK, Thompson EW, Brown TJ: Antisense-mediated suppression of hyaluronan synthase 2 inhibits the tumorigenesis and progression of breast cancer. Cancer Res 2005, 65:6139–6150
48. Itano N, Sawai T, Atsumi F, Miyaishi O, Taniguchi S, Kannagi R, Hamaguchi M, Kimata K: Selective expression and functional characteristics of three mammalian hyaluronan synthases in oncogenic malignant transformation. J Biol Chem 2004, 279:18679–18687
49. Tsuchiya N, Kondo Y, Takahashi A, Pawar H, Qian J, Sato K, Lieber MM, Jenkins RB: Mapping and gene expression profile of the minimally overrepresented 8q24 region in prostate cancer. Am J Pathol 2002, 160:1799–1806
50. Evanko SP, Parks WT, Wight TN: Intracellular hyaluronan in arterial smooth muscle cells: association with microtubules, RHAMM, and the mitotic spindle. J Histochem Cytochem 2004, 52:1525–1535
51. Evanko SP, Wight TN: Intracellular localization of hyaluronan in proliferating cells. J Histochem Cytochem 1999, 47:1331–1342
52. Lin G, Stern R: Plasma hyaluronidase (Hyal-1) promotes tumor cell cycling. Cancer Lett 2001, 163:95–101
53. Tammi R, Rilla K, Pienimaki JP, MacCallum DK, Hogg M, Luukkonen M, Hascall VC, Tammi M: Hyaluronan enters keratinocytes by a novel endocytic route for catabolism. J Biol Chem 2001, 276:35111–35122
54. Stern R: Devising a pathway for hyaluronan catabolism: are we there yet? Glycobiology 2003, 13:105R–115R
55. Stern R: Hyaluronan metabolism: a major paradox in cancer biology. Pathol Biol (Paris) 2005, 53:372–382
56. Stern R: Hyaluronan catabolism: a new metabolic pathway. Eur J Cell Biol 2004, 83:317–325
57. Liu D, Pearlman E, Diaconu E, Guo K, Mori H, Haqqi T, Markowitz S, Willson J, Sy MS: Expression of hyaluronidase by tumor cells induces angiogenesis in vivo. Proc Natl Acad Sci USA: 1996, 93:7832–7837
58. Lees VC, Fan TP, West DC: Angiogenesis in a delayed revascularization model is accelerated by angiogenic oligosaccharides of hyaluronan. Lab Invest 1995, 73:259–266
59. Rooney P, Kumar S, Ponting J, Wang M: The role of hyaluronan in tumour neovascularization [review]. Int J Cancer 1995, 60:632–636
60. Udabage L, Brownlee GR, Nilsson SK, Brown TJ: The over-expression of HAS2, Hyal-2 and CD44 is implicated in the invasiveness of breast cancer. Exp Cell Res 2005, 310:205–217
61. Asteriou T, Vincent JC, Tranchepain F, Deschrevel B: Inhibition of hyaluronan hydrolysis catalysed by hyaluronidase at high substrate concentration and low ionic strength. Matrix Biol 2006, 25:166–174